Fabrication of Nanometer-Sized Protein Patterns Using Atomic Force Microscopy and Selective Immobilization

Kapila Wadu-Mesthrige, Nabil A. Amro, Jayne C. Garno, Song Xu, and Gang-yu Liu
Department of Chemistry, Wayne State University, Detroit, Michigan 48202 USA

ABSTRACT A new methodology is introduced to produce nanometer-sized protein patterns. The approach includes two main steps, nanopatterning of self-assembled monolayers using atomic force microscopy (AFM)-based nanolithography and subsequent selective immobilization of proteins on the patterned monolayers. The resulting templates and protein patterns are characterized in situ using AFM. Compared with conventional protein fabrication methods, this approach is able to produce smaller patterns with higher spatial precision. In addition, fabrication and characterization are completed in near physiological conditions. The adsorption configuration and bioreactivity of the proteins within the nanopatterns are also studied in situ.

INTRODUCTION

Micropatterns of bioreceptors such as DNA, proteins, and oligonucleotides have revolutionized the life science and pharmaceutical industries (Nicolini, 1995). Microfabricated DNA chips or DNA microarrays have been used to measure expression levels of genes in plant, yeast, and human samples (Schena et al., 1996; Ramsy, 1998; Cairney et al., 1999). Many diseases can be diagnosed using DNA or protein microarrays (Blawas and Reichert, 1998; Wittstock et al., 1998; Edelstein et al., 2000). Microarrays using fluorescent probes are widely used to screen a large number of compounds produced using combinatorial chemistry and to identify potential drugs for the pharmaceutical industry (Fodor et al., 1991). Further miniaturization of these bioarrays or biochips offers the reward of higher density. More importantly, by nanofabrication of bioreceptors, one may be able to influence or control bioreactions, since the dimension of the bioentities such as proteins is on the order of nanometers. One prospective application is to regulate cell-extracellular matrix protein interactions by positioning these proteins on surfaces with nanometer precision.

Micropatterns as small as 300 nm can be readily produced using well-known techniques. Frequently reported methods of microfabrication include photolithography (Hengsakul and Cass, 1996; Liu and Hlady, 1996; Bernard et al., 1998; Nicolau et al., 1998) and micromachining (Bergman et al., 1998). These techniques produce features as small as 1 μm. Recent advances in electron and argon ion beam lithography and microcontact printing have broken the wavelength barrier and produced patterns as small as 300 nm (Tiberio et al., 1993; Sondag-Huethorst et al., 1994; Mrksich et al., 1996; Bergman et al., 1998).

Production of patterns smaller than 100 nm requires new fabrication and characterization strategies. Scanning probe microcopy (SPM) such as scanning tunneling microscopy (STM) and atomic force microscopy (AFM) are well known for their capability to image materials with the highest spatial resolution (Binnig et al., 1986; Bottomley et al., 1996; Colton et al., 1997). Taking advantage of the sharpness of the tips and the strong and localized tip-surface interactions, SPM has also been used to produce nanometer-sized patterns on surfaces (Nyffenegger et al., 1997; Liu et al., 2000).

An alternative approach of nanofabrication involves the use of organic thin films with two or more components; one with reactive terminal groups, which can bind proteins, and the other one, which is biologically inert (Fang and Knobler, 1996; Fang et al., 1997). Typically, the two components are mixed in solution and then form a self-assembled monolayer (SAM) or a Langmuir-Blodgett (LB) film (Fang and Knobler, 1996; Fang et al., 1997). The resulting thin films consist of domains of bioactive molecules inlaid in nonreactive assemblies. The size of the reactive islands depends on the concentration and sample preparation conditions (Fang and Knobler, 1996; Fang et al., 1997). Proteins can then be immobilized onto these domains via physical interactions (Mooney et al., 1996; Lestelius et al., 1997; Buijs et al., 1998; Nicolau et al., 1998), covalent binding (Norde et al., 1995; Vinckier et al., 1995; Wagner et al., 1996; Silin et al., 1997) or biospecific linkage (Lee et al., 1994; Houseman and Mrksich, 1998; Dontha et al., 1999; Mrksich, 2000). This approach is simple, although it suffers a disadvantage that the distribution and size of the receptor islands are determined by the interplay between the kinetics and thermodynamics of self-assembly and protein adsorption on SAMs.

In this article, we report our approach in producing protein nanopatterns with precise control over the pattern size and geometry. The basic idea of our approach is to use SAMs as nanometer thickness resists. Two-dimensional nanopatterns of SAMs are produced using scanning probe

Received for publication 12 September 2000 and in final form 16 January 2001.

Address reprint requests to Dr. Gang-yu Liu, Department of Chemistry, Wayne State University, 5101 Cass Avenue, Detroit, MI 48202. Tel.: 313-577-8658; Fax: 313-577-8822; E-mail: gyl@chem.wayne.edu.

0006-3495/01/04/1891/09 $2.00

lithography (SPL). These prepatterned SAMs will dictate the subsequent adsorption of proteins. The structure of resists and protein patterns and their bioactivity will be studied in situ using AFM.

MATERIALS AND METHODS

Preparation of self-assembled monolayers

The compounds 1-hexanethiol ($HS(CH_2)_5CH_3$, 95% purity), 1-decanethiol, ($HS(CH_2)_9CH_3$, 96% purity) 1-dodecanethiol ($HS(CH_2)_{11}CH_3$, 96% purity), and 2-mercapto-1-propanoic acid ($HS(CH_2)_2COOH$, 97%) were purchased from Aldrich (St. Louis, MO). Compounds of 3-mercapto-1-propanal ($HS(CH_2)_2CHO$), 11-mercapto-1-undecanal ($HS(CH_2)_{10}CHO$), and 16-mercapto-1-hexadecanoic acid ($HS(CH_2)_{15}COOH$) were synthesized following the procedures reported previously (Corey and Schmidt, 1979; Bain et al., 1989). Ultraflat gold films, 150 nm in thickness, were prepared according to the method developed by Hegner (Hegner et al., 1993) and Wagner (Wagner et al., 1995). The resulting gold surfaces have a mean roughness of 2–5 Å according to our AFM measurements. Thiol self-assembled monolayers, (SAMs) were prepared by immersing the freshly prepared gold films into the corresponding thiol solutions (0.1 to 1.0 mM) for at least 18 h.

Protein solutions

Bovine serum albumin (BSA, fraction V, which is essentially fatty acid free), lysozyme (LYZ, from hen egg, 95% purity), rabbit immunoglobulin G (IgG, purity 95%), rabbit anti-BSA IgG and mouse anti-rabbit IgG were purchased from Sigma Biochemicals (St. Louis, MO) and used without further purification. The proteins were diluted to the desired concentrations with the corresponding buffer solutions.

Atomic force microscopy

The AFM used for this study incorporates a home-constructed, deflection-type scanner controlled by commercial electronics and software (RHK Technology, Inc., Troy, MI). The instrument allows simultaneous acquisition of multiple images such as topography, frictional force, and elasticity images. The scanner may be operated under ambient laboratory conditions, in vacuum, or in solution (Kolbe et al., 1992; Liu et al., 1994). The cantilevers made of Si_3N_4 were either sharpened microlevers from ThermoMicroscopes (Sunnyvale, CA) with a force constant of 0.1 N/m or standard microlevers from Digital Instruments (Santa Barbara, CA) with a force constant of 0.38 N/m. Images were acquired with a typical imaging force of 0.15 nN using contact mode imaging in liquid media. Under these imaging conditions, little perturbation is observed for adsorbed proteins on surfaces.

RESULTS AND DISCUSSION

Basic procedure of fabrication of nanometer-sized protein patterns

The success of our approach relies upon 1) production of nanometer-sized patterns of SAMs and then 2) selective adsorption of proteins onto these patterns. The quality of the protein nanostructures depends on the spatial precision of SAM nanopatterns and on the selectivity of protein adsorption. Patterned SAMs are produced with nanometer precision using nanografting, a technique that was developed and reported by our group (Xu and Liu, 1997; Xu et al., 1999). Selectivity of protein adsorption can be achieved with the knowledge of variation in protein affinity toward different SAMs (Prime et al., 1991; Frey et al., 1995; Norde et al., 1995; Vinckier et al., 1995; Wagner et al., 1996; Patel et al., 1997; Blawas et al., 1998; Buijs et al., 1998). It is known that SAMs terminated with oligo(ethylene glycol), or tri(propylene sulfoxide) can resist protein adsorption (Prime and Whitesides, 1993; Deng et al., 1996; Harder et al., 1998; McPherson et al., 1998) and thus are good candidates for matrix layers. In addition, we have found that many proteins exhibit very little adsorption onto methyl-terminated SAMs under specified conditions, e.g., when the solution pH value deviates sufficiently from the isoelectric point (IEP) of the proteins (Wadu-Mesthrige et al., 2000). Commonly used protein adhesive groups include carboxylic acid, aldehydes, and biotin, onto which proteins may attach via electrostatic interactions, covalent binding, and biospecific interactions, respectively (Tarlov et al., 1993; Lee et al., 1994; Wollman et al., 1994; Vinckier et al., 1995; Mooney et al., 1996; Wagner et al., 1996; Blawas et al., 1998; Dontha et al., 1999). Recently, SAMs terminated by short peptide ligands such as Arg-Gly-Asp tripeptide have been used to immobilize proteins and cells (Houseman and Mrksich, 1998; Pakalns et al., 1999; Mrksich, 2000).

Our procedure is illustrated in more detail in Fig. 1. Nanografting can produce patterns of SAMs with nanometer precision, and the molecules within these patterned areas are closely packed (Xu et al., 1998). Under a typical low load, e.g., 0.1–1.0 nN, methyl-terminated SAM matrices are imaged in solution (Fig. 1 *A*). A fabrication site is then selected, typically on a large flat terrace. When a higher force, e.g., 10–30 nN, is applied to the AFM tip during scanning (Fig. 1 *B*), the matrix molecules under the tip are displaced. New thiol molecules from the solution above assemble immediately onto the exposed Au(111) substrate, following the shaving track of the AFM tip. Under reduced imaging forces, the features are characterized in situ (Fig. 1 *C*). To produce protein patterns, the matrix layer comprises thiols that are protein non-adhesive, whereas the nanopatterned areas contain thiols with protein adhesive termini such as aldehyde and carboxylate (Wadu-Mesthrige et al., 1999). Under carefully chosen conditions, proteins selectively adsorb onto these nanopatterns. The selectivity of protein adsorption arises from the difference in the protein affinity toward the surfaces of SAMs, which can be regulated by varying the terminal groups and the immobilization conditions. We are able to control the conditions such that adsorption occurs primarily on the nanopatterns of SAMs containing reactive groups (e.g., aldehyde, carboxylate, or biotin) as shown in Fig. 1 *D*. Proteins that are weakly bound to the methyl-terminated areas are rinsed away with buffers or surfactant solutions. Using this method, nanopatterns of proteins have been fabricated with lateral dimensions ranging from 10 nm to 1 μm.

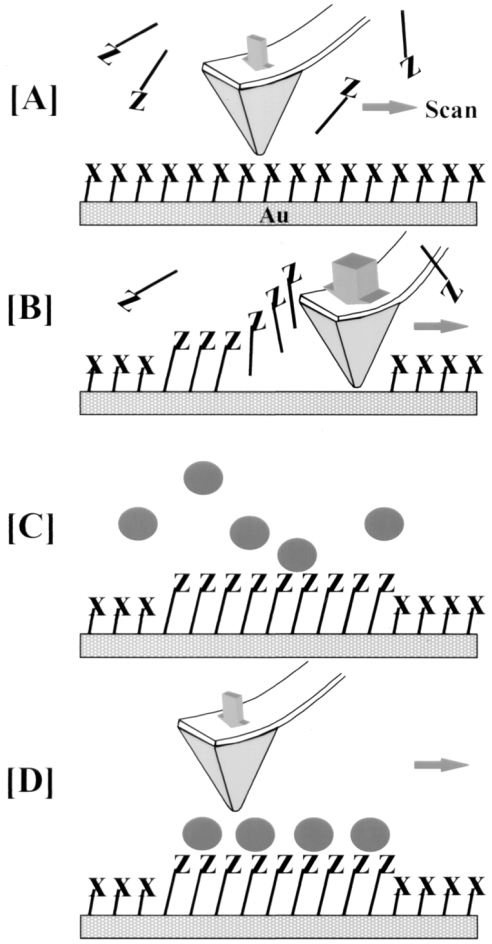

FIGURE 1 Schematic diagram illustrating the basic steps to produce nanometer-sized protein patterns. (*A*) The surface is imaged under low force, where X represents protein non-adhesive terminal groups such as methyl, and Z represents protein adhesive groups such as carboxylate or aldehyde. (*B*) Nanometer-size patterns of Z-termini are produced under high force using nanografting. (*C*) Proteins are selectively immobilized on the Z-terminated areas. (*D*) Protein nanopatterns are characterized by imaging under low force.

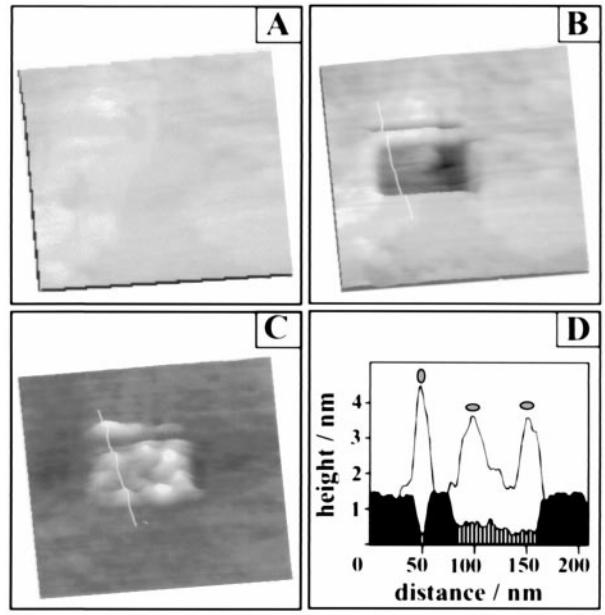

FIGURE 2 Nanopatterns of LYZ produced by immobilization of proteins via physisorption. (*A*) A 400 × 400 nm^2 area of a decanethiol SAM imaged under regular imaging force; (*B*) A 10 × 150 nm^2 line and a 100 × 150 nm^2 rectangle of 3-mercapto-1-propanoic acid nanografted within a 400 × 400 nm^2 area of a decanethiol SAM; (*C*) After subsequent 4-min immersion in a LYZ solution; (*D*) Corresponding cursor profile of the protein nanopatterns. In the cursor plots the origin is the gold surface determined by displacing SAM. The cursor profile on the corresponding patterned SAM is shown in the same plot. The black solid filled area represents undisturbed matrix SAM, the area filled with vertical lines follows the topography of the nanografted pattern from the white lines in image *B*, the white unfilled areas show the adsorbed protein, for the cursor line in *C*.

Producing nanopatterns of proteins via electrostatic interactions

As the first proof-of-concept experiment, lysozyme (LYZ) nanopatterns were produced via electrostatic immobilization. The decanethiol SAM on Au(111) was initially imaged in an aqueous solution containing 0.1 mM mercapto-propanoic acid as shown in Fig. 2 *A*. The image shows that the SAM has a smooth surface decorated by steps that correspond to single atomic Au(111) steps. The SAM nanopatterns are shown in Fig. 2 *B*, in which two patterns, a narrow line (10 × 150 nm^2) above a rectangle (100 × 150 nm^2), were grafted into a matrix. The two patterns are separated by 30 ± 5 nm. Both patterns exhibit negative contrast in the topographic image because the chain length of mercapto-propanoic acid is 0.5 ± 0.1 nm shorter than the matrix thiols. The fabrication and imaging of SAM nanopatterns were conducted in an aqueous medium containing 1 mM mercapto-propanoic acid. Next, the surface was rinsed thoroughly within the liquid cell to completely remove any residual thiols, first with deionized water and then with 20 mM HEPES buffer (pH 7.0). After rinsing, a 10 μg/ml solution of LYZ was injected. Within 3 min, proteins adsorbed exclusively onto the two patterned areas, as shown in Fig. 2 *C*. The high selectivity observed at pH 7 is mostly due to electrostatic attraction between the LYZ molecules and the carboxylate-terminated nanopatterns. Because the IEP of LYZ is 11.1 (Imoto et al., 1972), LYZ exhibits a net positive charge at pH 7. The pK_a value of mercapto-propanoic acid SAM is 8 (Hu and Bard, 1997), thus at neutral pH, ~10% of the nanopatterned area has a net negative charge. Consequently, the selectively of LYZ adsorption is mediated by electrostatic attraction. Under these conditions, little adsorption was observed at methyl-terminated areas within the time frame of the entire experiment (4 h). Furthermore, the boundary between the two nanopatterns remained clearly visible.

Individual LYZ particles can be resolved in the AFM image of Fig. 2 *C*. The corresponding cursor profiles in Fig.

2 *D* reveal that the immobilized protein molecules exhibit two different heights: 4.3 ± 0.2 nm and 3.0 ± 0.2 nm. It is known that physical interactions are not specific; therefore, various orientations with respect to the surface are observed for the adsorbed proteins. Because LYZ molecules are ellipsoidal with the approximate dimensions 4.5 × 3.0 × 3.0 nm^3 from x-ray crystallographic studies (Blake et al., 1965), the observed heights correspond to side-on and end-on orientations of LYZ, respectively.

Patterns of larger proteins such as rabbit immunoglobulin G (IgG) may also be produced using a similar approach with electrostatic interactions. We have succeeded in fabricating IgG patterns with lateral dimensions ranging from 100 to 250 nm. The apparent heights of IgG within nanopatterns are 3.8–6.2 nm (data not shown). The dimensions of IgG are 14.5 nm × 8.5 nm × 4.0 nm as determined by x-ray diffraction (Silverton et al., 1977). Therefore, the Y-shaped IgG molecules exhibit various orientations within the nanopatterns such as lying flat, side-on, and standing up.

Other than its experimental simplicity, physically mediated protein immobilization has several advantages. Many of the proteins retain their activity after immobilization onto carboxylate-terminated SAMs (Tarlov et al., 1993; Wollman et al., 1994; Mooney et al., 1996; Mrksich et al., 1996; Browning-Kelley et al., 1997). In addition, immobilization by electrostatic interactions is normally reversible. Thus, proteins can be removed by certain buffers or surfactants (Feng et al., 1996; Buijs et al., 1998), which can benefit applications that require the nanopatterns to be reusable.

Producing nanopatterns of proteins via covalent binding

For applications that require long-term stability, immobilization through specific interactions or covalent binding is more suitable. Well-known covalent immobilization involves the formation of disulfide, imine, or amide bonds (Vinckier et al., 1995; Baker et al., 1998). Fig. 3 shows three examples where nanopatterns were produced using covalent attachment. Fig. 3 *A* displays an AFM image of a 40 × 40 nm^2 area of mercapto-propanal grafted within a decanethiol SAM. The aldehyde pattern appears as a square hole in the matrix, with a depth of 0.5 ± 0.1 nm. After washing with water, a 5 μg/ml solution of IgG was injected into the liquid cell. The pH value of the protein solution was maintained at 6.5 using a HEPES buffer to ensure the formation of imine bonds between the surface aldehyde and the primary amine groups in the amino acids such as lysine in IgG. Because the IEP of IgG molecules ranges from pH 5–8, adsorption was observed on both the aldehyde and methyl-terminated areas at a solution pH of 6.5, within 5 min of soaking in protein solution. The adsorption of IgG on aldehyde-terminated areas results from the formation of imine bonds between the terminal aldehyde and the primary amino acid groups such as lysine at the surface of IgG. The adsorption of IgG on the methyl-terminated area is due to the hydrophobic interactions (Wadu-Mesthrige et al., 2000). After washing with 1% Tween 20 surfactant solution, the weakly adsorbed proteins on the methyl-terminated matrix areas detached completely, although the proteins covalently immobilized on the aldehyde-terminated area remained securely attached, as shown in Fig. 3 *B*. The cursor profile shown in Fig. 3 *C* reveals heights ranging from 4 to 6 nm for immobilized IgG molecules. The Y-shaped IgG (Silverton et al., 1977) can adopt several possible orientations due to the presence of several lysine residues. The possible configurations are depicted in Fig. 3 *C* as well.

For the covalent immobilization of LYZ, a positive 350 × 300 nm^2 pattern (Fig. 3 *D*) was produced within a hexanethiol matrix using an aldehyde-terminated thiol with a longer chain, mercapto-undecanal. Due to the low solubility of this thiol in water, sec-butanol was used as the solvent. After nanografting, the sample was rinsed copiously with ethanol followed by deionized water to change the media from organic to aqueous phase. This procedure requires a highly stable AFM configuration to prevent drifting away from areas containing nanopatterns. At pH 7, LYZ has a net positive charge and thus did not attach to the hydrophobic matrix SAM. Instead, LYZ adsorbs exclusively onto the 300 × 300 nm^2 aldehyde-terminated area via covalent binding as shown in Fig. 3 *E*. Individual protein molecules can be resolved from the AFM image. More importantly, the orientation of each immobilized protein is revealed from the topographic image (Fig. 3 *E*) and the corresponding cursor profile in Fig. 3 *F*. The LYZ molecules in the nanopattern exhibit various orientations, likely due to the multiple amine-containing residues in each protein. Although covalent immobilization involves more steps technically, proteins covalently bonded on nanopatterns are much more stable than proteins immobilized by physisorption when subjected to washing with water, buffer, and surfactant solutions.

Smaller proteins can also be patterned using similar procedures. A bovine serum albumin (BSA) pattern is shown in Fig. 3 *G*. A 200 × 250 nm^2 negative pattern similar to Fig. 3 *A* was produced within a hexanethiol matrix using mercapto-propanal. Again, the sample area was washed thoroughly with deionized water, and then the medium was replaced with a pH 6.5 HEPES buffer solution containing 10 μg/ml BSA. After ~3 min of immersion, a near monolayer of BSA was observed exclusively on the aldehyde-terminated negative pattern, as shown in Fig. 3 *H*. The adsorption of BSA onto the methyl-terminated matrix is negligible under these experimental conditions. The BSA molecules may adsorb individually or as aggregates. The heights measured for individual BSA as shown by the cursor plots in Fig. 3 *I* are consistent with the known dimensions of BSA, approximately spherical in shape with a diameter of 3.5 nm (Rosenoer et al., 1977).

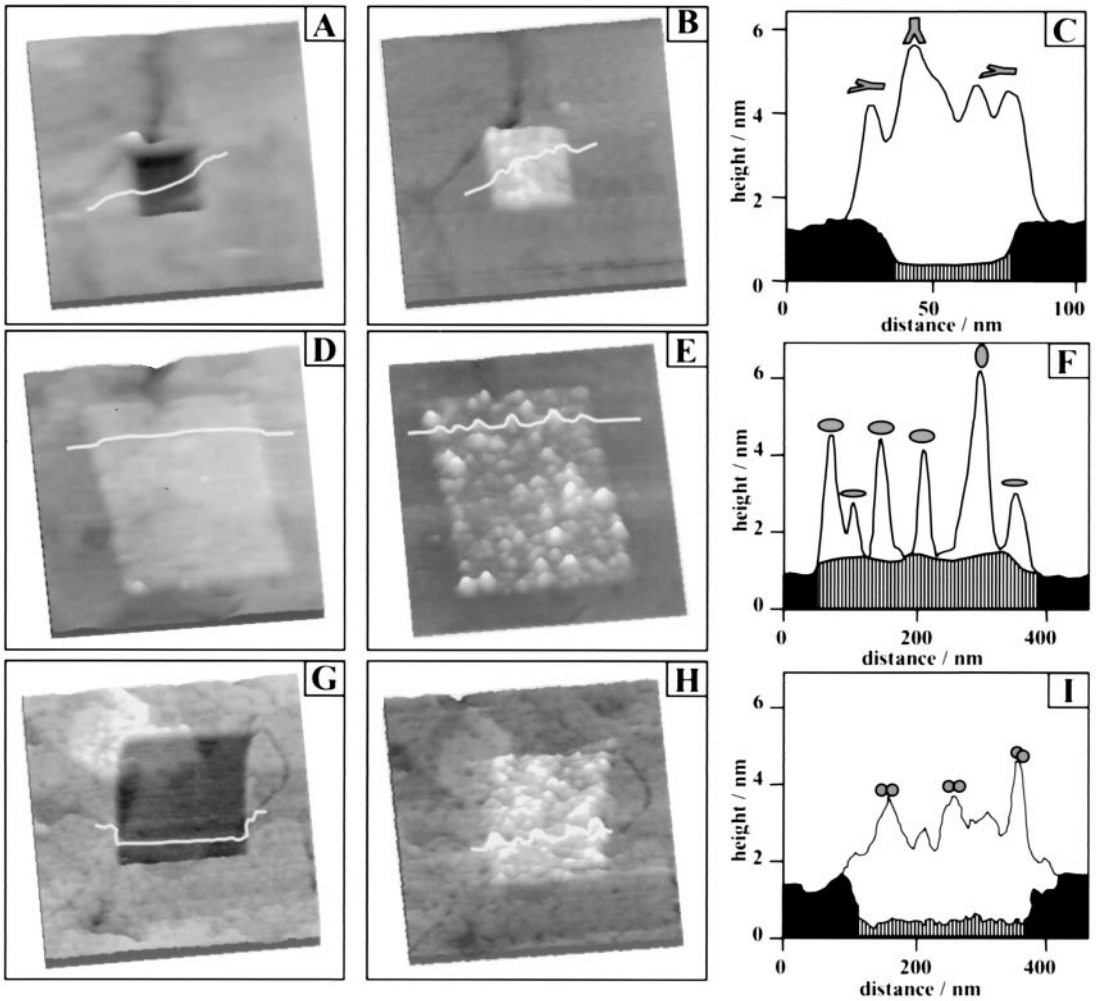

FIGURE 3 Production of nanopatterns of IgG, LYZ, and BSA via covalent binding. (*A*) A 150 × 150 nm^2 topographic image with a 40 × 40 nm^2 pattern of 3-mercapto-1-propanal in a decanethiol SAM matrix; (*B*) The same pattern after IgG adsorption; (*C*) The combined cursor profile of images *A* and *B*; (*D*) A 600 × 600 nm^2 topographic image of a hexanethiol SAM matrix, with a 350 × 300 nm^2 nanografted pattern of 11-mercapto-1-undecanal; (*E*) The same area imaged after LYZ adsorption; (*F*) The combined cursor profile of images *D* and *E*; (*G*) A 600 × 600 nm^2 topographic image of a hexanethiol SAM, with a 200 × 250 nm^2 nanopattern of 3-mercapto-1-propanal; (*H*) The same area imaged after immobilization of BSA; (*I*) The combined cursor profile of *G* and *H*.

Reactivity and stability of the nanopatterns of proteins

We have shown, in our previous studies using in situ and real-time AFM imaging, that tobacco mosaic virus capsid proteins, tobacco etch virus capsid proteins, and BSA can bind antibodies specifically after immobilization on carboxylic acid terminated SAMs (Browning-Kelly et al., 1997). This observation is consistent with the results from other research labs using fluorescence microscopy (Lestelius et al., 1997; Jones et al., 1998; Lahiri et al., 1999). The binding of specific IgG with electrostatically immobilized antigens on SAMs functionalized with —$O(CO)CF_3$, —OSO_3H, and —COOH has been demonstrated using ellipsometry, fluorescent confocal scanning laser microscopy, and AFM (Lestelius et al., 1997; Jones et al., 1998). However, for more strongly bound proteins, such as with covalent immobilization, the probability of denaturation may increase.

We tested the reactivity of protein nanopatterns produced via covalent immobilization. Fig. 4 *A* shows an example in which the bioactivity of immobilized rabbit IgG was tested by their reactivity toward mouse anti-rabbit IgG. In Fig. 4 *A*, several aldehyde-terminated nanopatterns, a1–a5, were first grafted with sizes 440 × 180 nm^2, 200 × 180 nm^2, 300 × 180 nm^2, 250 × 250 nm^2, and 300 × 300 nm^2, respectively. The matrix is a dodecanethiol SAM. The depth of these negative patterns is 0.8 ± 0.2 nm, in good agreement with the theoretical height difference between the two SAMs. The pattern in the lower right corner, a6, contains mixed dodecanethiol and mercaptopropanal SAM, resulting from incomplete removal of matrix SAM during nanografting.

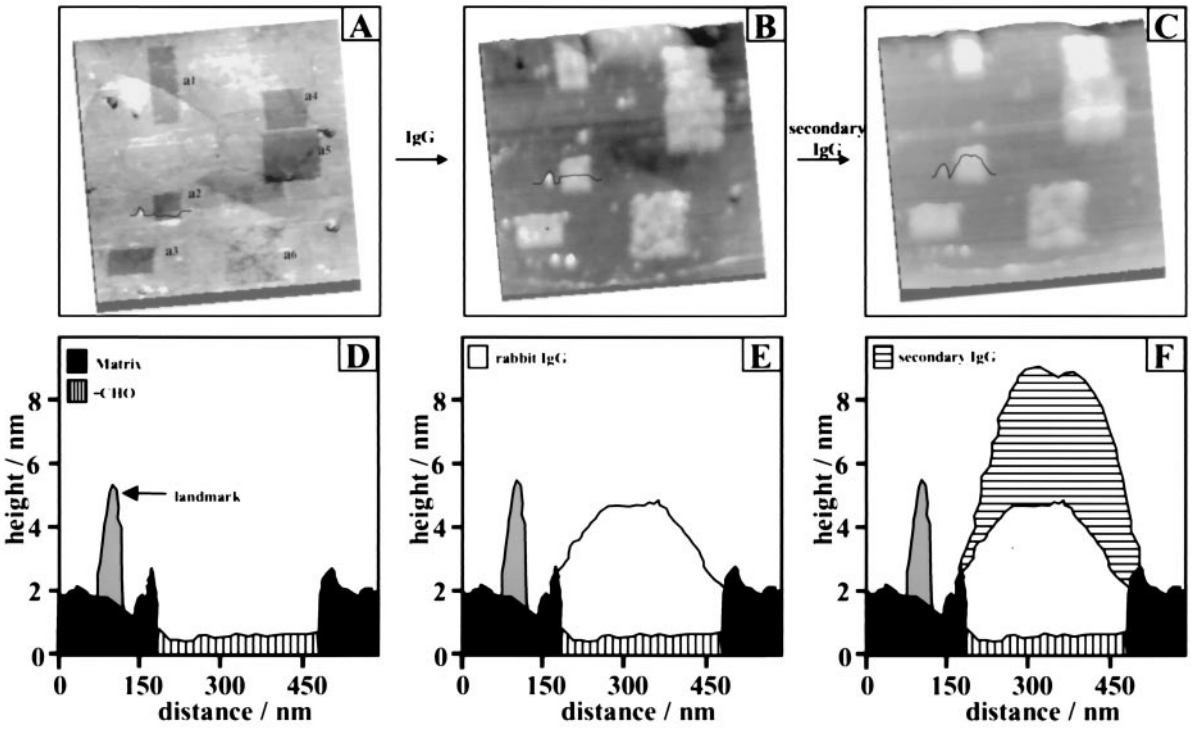

FIGURE 4 Recognition (binding) of specific mouse-anti-rabbit IgG onto nanopatterns of rabbit IgG. (*A*) Nanopatterns of 3-mercapto-1-propanal with sizes 500 × 200 nm^2, 200 × 200 nm^2, 300 × 180 nm^2, 300 × 300 nm^2, and 350 × 350 nm^2, a1–a5, were produced within a 1500 × 1500 nm^2 area of 1-dodecanethiol SAM. An incomplete pattern formed by using a smaller fabrication force is shown in the bottom right corner, a6. (*B*) The same area after the patterns were immersed in a 0.01 mg/ml solution of rabbit IgG for 3 min followed by washing with 1% Tween 20 solution. (*C*) After introducing mouse anti-rabbit IgG, the patterns display an increase in height, indicating the specific binding of antibody to the immobilized protein. (*D–F*) Corresponding cursor profiles drawn in the same position for images *A–C*. The feature (colored gray) beside pattern a2 is used as a reference to illustrate the height increases after rabbit IgG adsorption and after binding of mouse anti-rabbit IgG.

About 40% of pattern a6 consists of mercaptopropanal SAM. Within 5 min of injecting a 0.01 mg/ml solution of rabbit IgG (PBS buffer), adsorption was observed on all six of the aldehyde-terminated patterns and the matrix area. The IgG molecules on methyl-terminated matrix were removed easily by rinsing with a surfactant solution (1% Tween 20), resulting in highly stable immobilization as shown in Fig. 4 *B*. Rabbit IgGs in solution were completely removed before injecting mouse anti-rabbit IgG. Fig. 4 *C* shows the images 5 min after immersion in the secondary IgG solution.

By comparing the height of nanopatterns before and after secondary IgG injection, we conclude that antibody-antigen binding did occur. The height of the nanopatterns may be more quantitatively illustrated from the cursor profiles in Fig. 4, *D–F*. A sharp feature near a2, 3.6 ± 0.3 nm taller (gray area in Fig. 4 *D*) than the surrounding matrix, is used as a height reference. In Fig. 4 *E*, pattern a2 grew taller by 4.2 ± 0.2 nm upon the adsorption of rabbit IgG. This height increase is consistent with the expectation that each antibody has 57 lysine residues containing amines (the amino acid sequence of IgG was obtained from the Internet protein data bank at Brookhaven National Laboratories, PDB ID code 1IGT). Thus immobilized IgG may adopt various configurations after reacting with aldehyde. Resolving individual IgGs was not possible for such a large scan area (1600 × 1600 nm^2). After immersion in a solution of mouse anti-rabbit IgG, the height of all patterns increased by ~4.2–9.2 nm, indicating the attachment of secondary antibody. Such a wide height range is expected because the rabbit IgG molecules within the nanopatterns have various orientations on surfaces. The end of the F_c fragment of each rabbit IgG serves as the binding site for the mouse anti-rabbit IgG. The ends of the F_{ab} fragment of the Y-shaped mouse anti-rabbit IgG binds specifically to the rabbit IgG. Various orientations of the rabbit IgG lead to different configurations of the antibody-antigen binding complexes, which result in height increases ranging from 4.2 to 9.2 nm for the nanopatterns. Several possible orientations of binding are shown in Fig. 5. We emphasize that the binding is biospecific because little adsorption was observed when nonspecific antibodies were used. A more definitive conclusion requires the design and completion of an activity assay using nanopatterns of proteins.

In biosensors and bioanalytical devices, immobilized proteins are often subject to subsequent washing with water, buffer, and surfactant solutions (Feng et al., 1996; You and

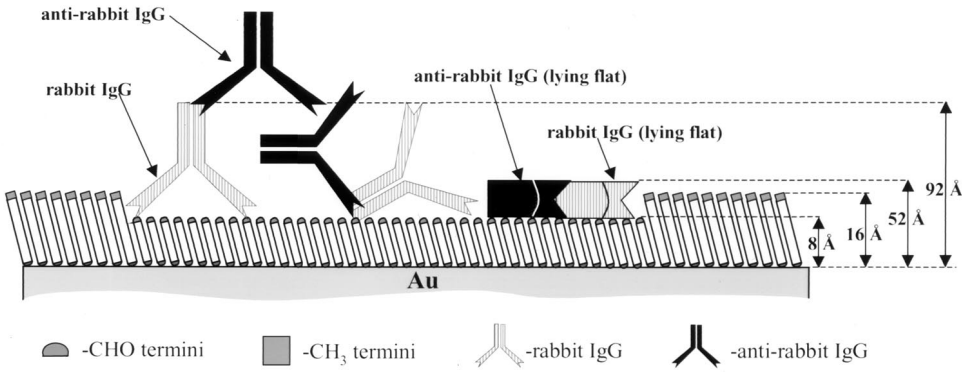

FIGURE 5 Three possible orientations for rabbit IgG within nanopatterns and their recognition by the secondary IgG. The heights with respect to the Au (111) surface are indicated to facilitate understanding the observed height increases for the experiment shown in Fig. 4.

Lowe, 1996). The stability of immobilized proteins toward various chemical treatments was investigated by washing the protein patterns and imaging under the chosen solutions for a long time. Three solutions were used for these tests: deionized water, buffer solutions, and 1% Tween 20, a non-ionic surfactant. For the protein patterns tested, all can sustain washing by pure water and buffer solutions. Under 1% Tween 20 solution, the physically immobilized proteins desorb, whereas the BSA, LYZ, and IgG molecules immobilized on aldehyde-terminated SAM patterns do not detach. This washing procedure eliminates any loosely bound biomolecules on SAMs.

The binding strength of proteins within nanopatterns may be estimated semi-quantitatively, by continuous AFM imaging while increasing the imaging force. The immobilized proteins on SAM nanopatterns can sustain pressure (~0.01 GPa) exerted by the tip during regular contact-mode imaging. If the load is increased beyond a certain threshold, protein may be displaced from SAM nanopatterns. The measured force threshold for the proteins (immobilized via electrostatic interactions) falls in the range of 12 to 30 nN (~0.21–0.52 GPa, respectively), whereas protein immobilized via covalent binding cannot be removed until the force is increased beyond 70 nN (~1.2 GPa).

CONCLUSION

We introduce a new approach to fabricate and characterize nanometer-sized protein patterns with precise control over the pattern size and geometry. The AFM experiments presented in this report demonstrate an unprecedented level of control in the placement and arrangement of protein receptors on surfaces, achievable at a scale of tens of nanometers. Individual proteins are resolved and their orientations on nanopatterns revealed. Most proteins within nanopatterns remain active as demonstrated by their binding to specific antibodies. This technique has the potential to manipulate individual protein molecules with angstrom precision. The main advantages include 1) ability to produce nanometer-sized patterns of bioreceptors, 2) high spatial precision, and 3) imaging and fabrication performed in situ and under near physiological conditions. The methodology developed here is generic. Although not yet practical for high-throughput applications and manufacturing, this approach provides a unique opportunity for exploration of chemical and biochemical reactions, such as cell-extracellular matrix protein interactions, under spatially well-defined and controlled environments.

We appreciate many helpful discussions with Sylvain Cruchon-Dupeyrat, Joey Oravec, and Dr. V. Hari at Wayne State University.
This research was supported by the Whitaker Foundation (Biomedical Engineering grant) and the National Science Foundation (9733400 and 9870720).

REFERENCES

Bain, C. D., E. B. Troughton, Y. Tao, J. Evall, G. M. Whitesides, and R. G. Nuzzo. 1989. Formation of monolayer films by the spontaneous assembly of organic thiols from solution onto gold. *J. Am. Chem. Soc.* 111:321–335.

Baker, A., L. Zidek, D. Wiesler, J. Chmelik, M. Pagel, and M. V. Novotny. 1998. Reaction of *N*-acetylglycyllysine methyl ester with 2-alkenals: an alternative model for covalent modification of proteins. *Chem. Res. Toxicol.* 11:730–740.

Bergman, A. A., J. Buijs, J. Herbig, D. T. Mathes, J. J. Demarest, C. D. Wilson, C. T. Reimann, R. A. Baragiola, R. Hull, and S. O. Oscarsson. 1998. Nanometer-scale arrangement of human serum albumin by adsorption on defect arrays created with a finely focused ion beam. *Langmuir.* 14:6785–6788.

Bernard, A., E. Delamarche, H. Schmid, B. Michel, H. R. Bosshard, and H. Biebuyck. 1998. Printing patterns of proteins. *Langmuir.* 14:2225–2229.

Binnig, G., C. F. Quate, and C. Gerber. 1986. Atomic force microscope. *Phys. Rev. Lett.* 56:930–933.

Blake, C. C. F., D. F. Koenig, G. A. Mair, A. C. T. North, D. C. Phillips, and V. R. Sarma. 206. 1965. Structure of hen egg-white lysozyme. *Nature.*757–761.

Blawas, A. S., T. F. Oliver, M. C. Pirrung, and W. M. Reichert. 1998. Step-and-repeat photopatterning of protein features using caged-biotin-BSA: characterization and resolution. *Langmuir.* 14:4243–4250.

Blawas, A. S., and W. M. Reichert. 1998. Protein patterning. *Biomaterials.* 19:595–609.

Bottomley, L. A., J. E. Coury, and P. N. First. 1996. Scanning probe microscopy. *Anal. Chem.* 68:185R–230R.

Browning-Kelley, M. E., K. Wadu-Mesthrige, V. Hari, and G.-Y. Liu. 1997. Atomic force microscopic study of specific antigen/antibody binding. *Langmuir.* 13:343–350.

Buijs, J., D. W. Britt, and V. Hlady. 1998. Human growth hormone adsorption kinetics and conformation on self-assembled monolayers. *Langmuir.* 14:335–341.

Cairney, J., N. F. Xu, G. S. Pullman, V. T. Ciavatta, and B. Johns. 1999. Natural and somatic embryo development in loblolly pine gene expression studies using differential display and DNA arrays. *Appl. Biochem. Biotechnol.* 5:77–79.

Colton, R. J., D. R. Baselt, Y. F. Dufrene, J. B. D. Green, and G. U. Lee. 1997. Scanning probe microscopy. *Curr. Opin. Chem. Biol.* 1:370–377.

Corey, E. J., and G. Schmidt. 1979. Useful procedures for the oxidation of alcohols involving pyridinium dichromate in aprotic media. *Tetrahedron Lett.* 5:399–402.

Deng, L., M. Mrksich, and G. M. Whitesides. 1996. Self-assembled monolayers of alkanethiolates presenting tri(propylene sulfoxide) groups resist the adsorption of protein. *J. Am. Chem. Soc.* 118:5136–5137.

Dontha, N., W. B. Nowal, and W. G. Kuhr. 1999. Development of sub-micron patterned carbon electrodes for immunoassays. *J. Pharmacol. Biomed. Anal.* 19:83–91.

Edelstein, R. L., C. R. Tamanaha, P. E. Sheehan, M. M. Miller, D. R. Baselt, L. J. Whitman, and R. J. Colton. 2000. The BARC biosensor applied to the detection of biological warfare agents. *Biosensors Bioelectronics.* 14:805–813.

Fang, J., and C. M. Knobler. 1996. Phase-separated two-component self-assembled organosilane monolayers and their use in selective adsorption of a protein. *Langmuir.* 12:1368–1374.

Fang, J., C. M. Knobler, M. Gingery, and F. A. Eiserling. 1997. Imaging bacteriophage T4 on patterned organosilane monolayers by scanning force microscopy. *J. Phys. Chem. B.* 101:8692–8695.

Feng, M., A. B. Morales, T. Beugeling, A. Bantjes, K. vanderWerf, G. Gosselink, B. deGrooth, and J. Greve. 1996. Adsorption of high density lipoproteins (HDL) on solid surfaces. *J. Colloid Interface Sci.* 177: 364–371.

Fodor, S. P. A., J. Leighton Read, M. C. Pirrung, L. Stryer, A. T. Lu, and D. Solas. 1991. Light-directed, spatially addressable parallel chemical synthesis. *Science.* 251:767–772.

Frey, B. L., C. E. Jordan, S. Kornguth, and R. M. Corn. 1995. Control of the specific adsorption of proteins onto cold surfaces with poly(L-lysine) monolayers. *Anal. Chem.* 67:4452–4457.

Harder, P., M. Grunze, R. Dahint, G. M. Whitesides, and P. E. Laibinis. 1998. Molecular conformation in oligo(ethylene glycol)-terminated self-assembled monolayers on gold and silver surfaces determines their ability to resist protein adsorption. *J. Phys. Chem. B.* 102:426–436.

Hegner, M., P. Wagner, and G. Semenza. 1993. Ultralarge atomically flat template-stripped Au surfaces for scanning probe microscopy. *Surf. Sci.* 291:39–46.

Hengsakul, M., and A. E. G. Cass. 1996. Protein patterning with a photoactivatable derivative of biotin. *Bioconjugate Chem.* 7:249–254.

Houseman, B. T., and M. Mrksich. 1998. Efficient solid-phase synthesis of peptide-substituted alkanethiols for the preparation of substrates that supports the adhesion of cells. *J. Org. Chem.* 63:7552–7555.

Hu, K., and A. J. Bard. 1997. Use of atomic force microscopy for the study of surface acid-base properties of carboxylic acid-terminated self-assembled monolayers. *Langmuir.* 13: 5114–5119.

Imoto, T., L. N. Johnson, A. C. T. North, D. C. Philips, and J. A. Rupley. 1972. Vertebrate lysozymes. *In* The Enzymes, 3rd ed, Vol. 7. P. D. Boyer, editor. Academic Press, New York. 665–868.

Jones, V. W., J. R. Kenseth, M. D. Porter, C. L. Mosher, and E. Henderson. 1998. Microminiaturized immunoassays using atomic force microscopy and compositionally patterned antigen arrays. *Anal. Chem.* 70: 12333–1241.

Kolbe, W. F., D. F. Ogletree, and M. B. Salmeron. 1992. Atomic force microscopy imaging of T4 bacteriophages on silicon substrates. *Ultramicroscopy.* 42:1113–1117.

Lahiri, J., E. Ostuni, and G. M. Whitesides. 1999. Patterning ligands on reactive SAMs by microcontact printing. *Langmuir.* 15:2055–2060.

Lee, G. U., D. A. Kidwell, and R. J. Colton. 1994. Sensing discrete streptavidin biotin interactions with atomic-force microscopy. *Langmuir.* 10:354–357.

Lestelius, M. B. Liedberg, and P. Tengvall. 1997. In vitro plasma protein adsorption on ω-functionalized alkanethiolate self-assembled monolayers. *Langmuir.* 13:5900–5908.

Liu, G.-Y., P. Fenter, C. E. D. Chidsey, D. F. Ogletree, P. Eisenberger, and M. Salmeron. 1994. An unexpected packing of fluorinated *n*-alkane thiols on Au(111): a combined atomic-force microscopy and x-ray diffraction study. *J. Chem. Phys.* 101:4301–4306.

Liu, J., and V. Hlady. 1996. Chemical pattern on silica surface prepared by UV irradiation of 3-mercaptopropyltriethoxy silane layer: surface characterization and fibrinogen adsorption. *Colloids Surfaces B Biointerfaces.* 8:25–37.

Liu, G.-Y., S. Xu, and Y. Qian. 2000. Nanofabrication of self-assembled monolayers using scanning probe lithography. *Acc. Chem. Res.* 33: 457–466.

McPherson, T., A. Kidane, I. Szleifer, and K. Park. 1998. Prevention of protein adsorption by tethered poly(ethylene oxide) layers: experiments and single-chain mean-field analysis. *Langmuir.* 14:176–186.

Mooney, J. F., A. J. Hunt, J. R. McIntosh, C. A. Liberko, D. M. Walba, and C. T. Rogers. 1996. Patterning of functional antibodies and other proteins by photolithography of silane monolayers. *Proc. Natl. Acad. Sci. U.S.A.* 93:12287–12291.

Mrksich, M. 2000. A surface chemistry approach to study cell adhesion. *Chem. Soc. Rev.* 29:267–273.

Mrksich, M., C. S. Chen, Y. Xia, L. E. Dike, D. E. Ingber, and G. M. Whitesides. 1996. Controlling cell attachment on contoured surfaces with self-assembled monolayers of alkanethiolates on gold. *Proc. Natl. Acad. Sci. U.S.A.* 93:10775–10778.

Nicolau, D. V., T. Taguchi, H. Taniguchi, and S. Yoshikawa. 1998. Micron-sized protein patterning on diazonaphthoquinone/novolak thin polymeric films. *Langmuir.* 14:1927–1936.

Nicolini, C. 1995. From neural chip and engineered biomolecules to bioelectronic devices: an overview. *Biosensors Bioelectronics.* 10: 105–127.

Norde, W., M. Giesbers, and H. Pingsheng. 1995. Langmuir-Blodgett films of polymerized 10,12-pentacosadiyonic acid as substrates for protein adsorption. *Colloids Surfaces B Biointerfaces.* 5:255–263.

Nyffenegger, R. M., and R. M. Penner. 1997. Nanometer-scale surface modification using the scanning probe microscope: progress since 1991. *Chem. Rev.* 97:1195.

Pakalns, T., K. L. Haverstick, G. B. Fields, J. B. McCarthy, D. L. Mooradian, and M. Tirrell. 1999. Cellular recognition of synthetic peptide amphiphiles in self-assembled monolayer films. *Biomaterials.* 20: 2265–2279.

Patel, N., M. C. Davies, M. Hartshorne, R. J. Heaton, C. J. Roberts, S. J. B. Tendler, and P. M. Williams. 1997. Immobilization of protein molecules onto homogeneous and mixed carboxylate-terminated self-assembled monolayers. *Langmuir.* 13:6485–6490.

Prime, K. L., and G. M. Whitesides. 1991. Self-assembled organic monolayers: model systems for studying adsorption of proteins at surfaces. *Science.* 252:1164–1167.

Prime, K. L., and G. M. Whitesides. 1993. Adsorption of proteins onto surfaces containing end-attached oligo(ethylene oxide): a model system using self-assembled monolayers. *J. Am. Chem. Soc.* 115:10714–10721.

Ramsy, G. 1998. DNA chips: state-of-the art. *Nat. Biotechnol.* 18:40.

Rosenoer, V. M., M. Oratz, and M. A. Rothschild. 1977. Albumin Function and Uses. Pergamon Press, New York.

Schena, M., D. Shalon, R. Heller, A. Chai, P. O. Brown, and R. W. Davis. 1996. Parallel human genome analysis: microarray-based expression monitoring of 1000 genes. *Proc. Natl. Acad. Sci. U.S.A.* 93: 10614–10619.

Silin, V., H. Weetall, and D. J. Vanderah. 1997. SPR studies of the nonspecific adsorption kinetics of human IgG and BSA on gold surfaces modified by self-assembled monolayers (SAMs). *J. Colloid Interface Sci.* 185:94–103.

Silverton, E. W., M. A. Navia, and D. R. Davies. 1977. Three-dimensional structure of an intact human immunoglobulin. *Proc. Natl. Acad. Sci. U.S.A.* 74:5140–5144.

Sondag-Huethorst, J. A. M., H. R. J. VanHelleputte, and L. G. J. Fokkink. 1994. Generation of electrochemically deposited metal patterns by means of electron-beam (nano)lithography of self-assembled monolayer resists. *Appl. Phys. Lett.* 64:285–287.

Tarlov, M. J., D. R. F. Burgess, and G. Gillen. 1993. UV photopatterning of alkanethiolate monolayers self-assembled on gold and silver. *J. Am. Chem. Soc.* 115:5305–5306.

Tiberio, R. C., H. G. Craighead, M. Lercel, T. Lau, C. W. Sheen, and D. L. Allara. 1993. Self-assembled monolayer electron beam resist on GaAs. *Appl. Phys. Lett.* 62:476–478.

Vinckier, A., I. Heyvaert, A. D'Hoore, T. McKittrick, C. Van Haesendonck, Y. Engelborghs, and L. Hellemans. 1995. Immobilizing and imaging microtubules by atomic force microscopy. *Ultramicroscopy.* 57: 337–343.

Wadu-Mesthrige, K., N. A. Amro, and G.-Y. Liu. 2000. Immobilization of proteins on self-assembled monolayers. *Scanning.* 22:380–388.

Wadu-Mesthrige, K., S. Xu, N. A. Amro, and G.-Y. Liu. 1999. Fabrication and imaging of nanometer-sized protein patterns. *Langmuir.* 15: 8580–8583.

Wagner, P., M. Hegner, H.-J. Guntherodt, and G. Semenza. 1995. Formation and in-situ modification of monolayers chemisorbed on ultraflat template-stripped gold surfaces. *Langmuir.* 11:3867–3875.

Wagner, P., M. Hegner, P. Kernen, F. Zaugg, and G. Semenza. 1996. Covalent immobilization of native biomolecules onto Au(111) via *N*-hydroxysuccinimide ester functionalized self-assembled monolayers for scanning probe microscopy. *Biophys. J.* 70:2052–2066.

Wittstock, G., S. H. Jenkins, H. B. Halsall, and W. R. Heineman. 1998. Continuing challenges for the immunoassay field. *Nanobiology.* 4:153–162.

Wollman, E. W., D. Kang, C. D. Frisbie, I. M. Lorkovic, and M. S. Wrighton. 1994. Photosensitive self-assembled monolayers on gold: photochemistry of surface-confined aryl azide and cyclopentadienylmanganese tricarbonyl. *J. Am. Chem. Soc.* 116:4395–4404.

Xu, S., P. E. Laibinis, and G.-Y. Liu. 1998. Accelerating the kinetics of thiol self-assembly on gold: a spatial confinement effect. *J. Am. Chem. Soc.* 120:9356–9361.

Xu, S., and G.-Y. Liu. 1997. Nanometer-scale fabrication by simultaneous nanoshaving and molecular self-assembly. *Langmuir.* 13:127–129.

Xu, S., S. Miller, P. E. Laibinis, and G.-Y. Liu. 1999. Fabrication of nanometer scale patterns within self-assembled monolayers by nanografting. *Langmuir.* 15:7244–7251.

You, H. X., and C. R. Lowe. 1996. AFM studies of protein adsorption. II. Characterization of immunoglobulin G: adsorption by detergent washing. *J. Colloid Interface Sci.* 182:586–601.